Electrocomponent Science and Technology
1977, Vol. 4, pp. 29–35

UHV – DEPOSITED AMORPHOUS TANTALUM AND TANTALUM–NICKEL FILMS

ALFRED SCHÄFER and GÜNTHER MENZEL†

Mitteilung aus dem Lehrstuhl für Metallurgie und Metallkunde der Technischen Universität München, Arcisstr. 21, FRG, und den Forschungslaboratorien München der Siemens AG, FRG

(Received April 6, 1977)

Tantalum produced by ultra-high vacuum vapour quenching has been identified on the basis of various forms of evidence as amorphous tantalum. Tantalum in this amorphous form has a resistivity of 230 $\mu\Omega$ cm and a temperature coefficient of resistivity (TCR) of −60 ppm/K. The films are stable below −90°C. At higher temperatures the amorphous structure suddenly turns into coarse-grained α tantalum.

Alloying with a mole fraction of 20% to 55% resulted in amorphous tantalum-nickel films with a temperature coefficient between −300 ppm/K and +500 ppm/K. The structure of the tantalum-nickel films, which are stable up to 300°C, was investigated by transmission electron microscopy.

Deposition of the tantalum on substrates heated to temperatures between −80°C and +150°C resulted in β tantalum, which turned into α tantalum between 160°C and 240°C. The appearance of positive and negative temperature coefficients in the amorphous films indicates that even in the amorphous state different conduction mechanisms may exist. According to the clean deposition conditions no influence of the residual gas on the film properties can be expected.

1. INTRODUCTION

Compared with polycrystalline films, amorphous metal films show different physical, especially electrical properties.[1] Most of the amorphous thin films investigated hitherto were deposited under high-vacuum conditions.[2-4] The possibility cannot be excluded that their resistivity and its associated TCR may be influenced by the incorporation of impurity atoms from the residual gas. In order to determine the exact relation between structural and electrical properties, metal films were deposited in ultra-high vacuum. The following points were of special interest:

1) Is it possible to produce amorphous non-alloyed metal films in UHV?

2) Over what temperature range does the amorphous structure remain stable?

3) Can the amorphous structure be stabilized by alloying with another ultra-pure metal?

The identification of the amorphous state was based on the following properties of the samples:[5-6]

- The films must show highly diffuse X-ray and electron diffraction patterns.
- Transmission electron microscopy with a resolution of about 1 nm may not resolve discrete grains of the samples.
- During heating of the films relatively large changes in the physical properties, especially of the electrical properties must occur within a narrow temperature range. Afterwards the samples must show a single-phase crystalline structure.

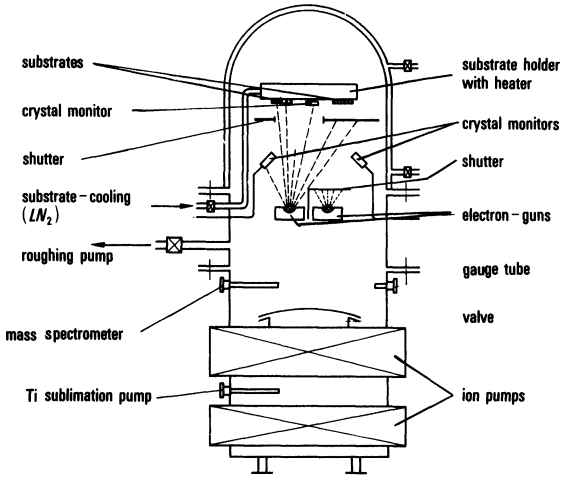

FIGURE 1 UHV deposition unit.

†Excerpt from doctoral dissertation of G. Menzel approved for advanced publication by the faculty of mechanical engineering of the Munich University of Technology.

2. UHV DEPOSITION TECHNIQUE

2.1. Equipment Used for Experiment

In order to produce amorphous metal films, the vapour quenching technique was chosen. A UHV evaporation unit as shown schematically in Figure 1 was employed for this purpose. Its oil-free pump station consists of two sorption pumps, a titanium sublimation pump and two noble gas stabilized ion getter pumps with a pumping rate of 700 l/s.

Two independent 6 kW electron-beam evaporators allowed the preparation of an alloy by the simultaneous evaporation of two metals. The deposition rate was automatically controlled by two water-cooled crystal oscillators, while a third crystal oscillator placed on the same level as the substrates determined the total thickness of the films. The copper substrate holder could be heated to 500°C and cooled to −160°C with liquid nitrogen. Six substrates (23 mm x 29 mm) could be fixed at the holder. The resistance of each sample could be measured as a function of temperature in UHV. A shutter below the substrate holder exposed only one substrate to the metal vapour at each deposition cycle.

The substrate temperature was measured via an NiCr–Ni thermocouple and the residual pressure via the ion current of the ion getter pumps and a Bayard-Alpert ionization guage.

The composition of the residual gas was analyzed with a mass spectrometer.

2.2 Performance of Experiment

The final residual pressure in the evaporation unit after four days of pumping and heat treatment at 250°C was 8.10^{-9} N/m^2 to 3.10^{-8} N/m^2. Analysis of the residual gas with the mass spectrometer disclosed no significant concentration of hydrocarbons or oxygen; the partial pressure of the water vapour and the nitrogen was less than 10^{-10} N/m^2. During the evaporation of the metal the pressure rose to between 9.10^{-8} N/m^2 and 8.10^{-7} N/m^2.

The materials evaporated were Marz grad tantalum (99.999%) and Marz grad nickel (99.999%), which were degassed prior to the deposition by repeated heat treatment and melting in UHV. The substrates, which were of Corningglas 7059, silica or beryllium oxide, had been degassed for six hours at 400°C at a pressure of 3.10^{-7} N/m^2.

The deposition rate at the substrates was 0.2 nm/s, while film thicknesses ranged between 45 nm and 80 nm.

2.3 Methods of Analyses

In order to investigate their structure and microstructure with a transmission electron microscope (Siemens ELMISKOP 101®) the films were detached directly from the substrates and prepared on diaphragms. The purity of the films was compared with that of the starting material by means of SIMS and Auger analyses. The composition of the tantalum-nickel films was checked by X-ray fluorescence analysis. Information on the structure and degree of order of the films yielded by electron diffractometry was supplemented by further data obtained by X-ray microstructure analysis. The film thickness was determined by a stylus method (Talystep) and by X-ray fluorescence analysis.

3. EXPERIMENTAL RESULTS

3.1. Pure Tantalum

Figure 2 shows the resistivity of a pure tantalum film (deposition temperature −160°C) as a function of the temperature. The resistivity after the deposition of the film is 230 μΩ cm and does not change significantly up to −90°C. Between −160°C and −90°C the film has a reversible TCR of $\alpha = -60$ ppm/K. Further heating causes an abrupt irreversible drop in resistivity which finishes at about −40°C. The continuous specific heat characteristic extending in the case of bulk and crystalline tantalum[5] from −263°C to

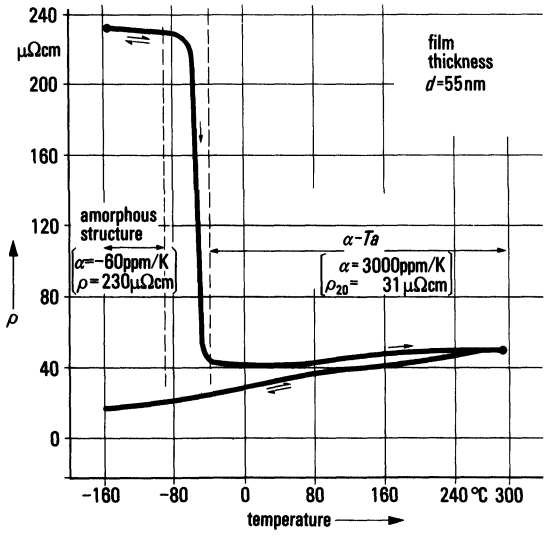

FIGURE 2 Resistivity ρ versus temperature of a tantalum thin film (deposition temperature −160°C).

+27°C shows that no phase transition, which would affect the conductivity, occurs in the bulk material. The drop in resistivity in the case of the thin tantalum films suggests therefore an additional structural change. Since the drop in resistivity is a definite indication of the existence of an amorphous phase,[5-6] it may be inferred that an amorphous tantalum phase exists over the temperature range of −160°C to −90°C.

Subsequent to its abrupt drop, the resistivity of the film exhibits up to 300°C a reversible characteristic with a TCR of +2000 ppm/K (temperature range 20°C to 300°C) and +3000 ppm/K (temperature range −160°C to 20°C), the resistivity now being $\rho_{20} = 31\ \mu\Omega$ cm. According to this result the transmission electron micrographs of these films reveal a very coarse-grained tantalum with an average grain size of about 50 μm (Figure 3).

Deposition temperature of −80°C to +150°C result in β tantalum with a grain diameter of 10 nm to 20 nm (Figure 4a). X-ray microstructure analyses and electron diffractometry exhibit a hexagonal structure for the β tantalum. In the electron diffraction pattern of Figure 4b some interplanar spacings of the single-phase β tantalum films are noted. The resistivity and TCR of these films ($\rho_{20} = 240\ \mu\Omega$ cm; $\alpha = -200$ ppm/K) agree well with the values given in the literature[8-9] for sputtered β tantalum films. As may be

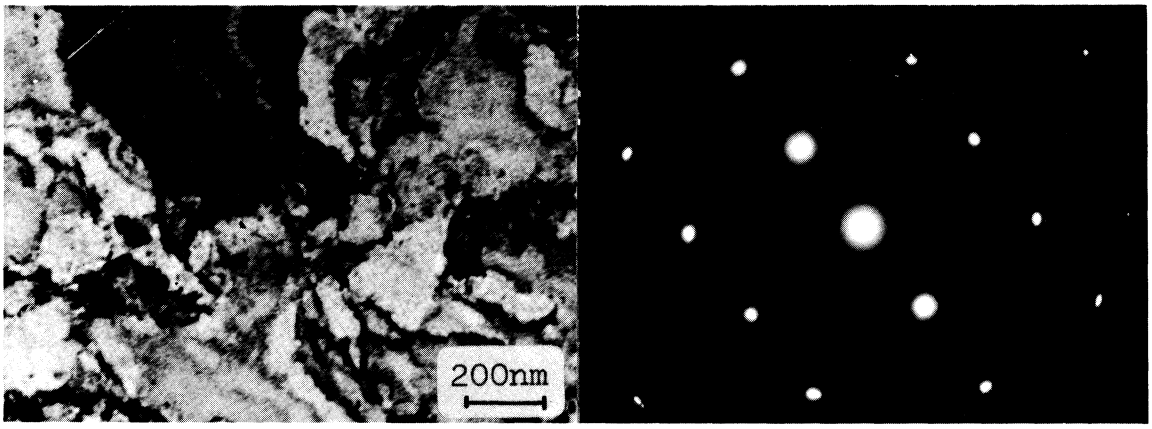

FIGURE 3 Transmission electron micrograph and diffraction pattern of an α tantalum thin film crystallized from the amorphous state (condensation temperature −160°C, heated to room temperature, film thickness d = 60 nm).

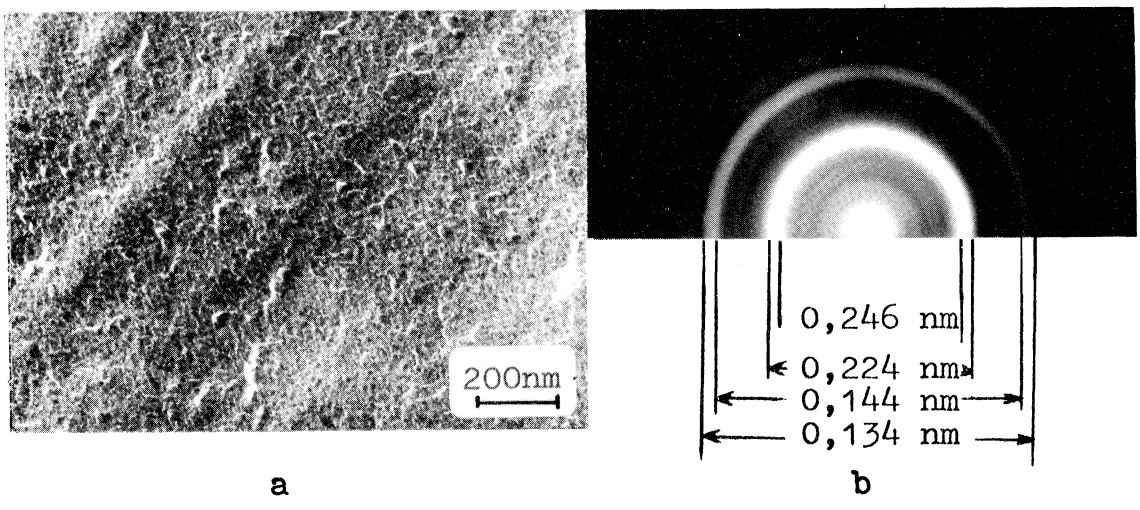

FIGURE 4 Transmission electron micrograph and diffraction pattern of a β tantalum thin film (condensation temperature 20°C, no heat treatment, film thickness d = 60 nm).

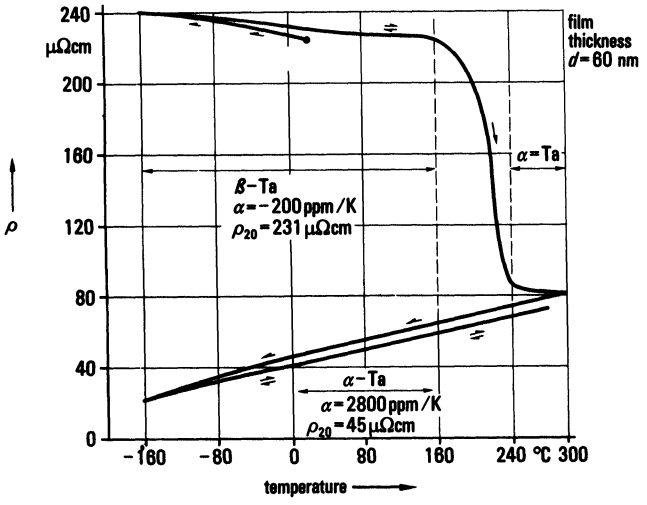

FIGURE 5 Resistivity ρ versus temperature of a tantalum film deposited at 20°C.

noted from Figure 5, in the case of UHV deposition, the transition of β tantalum to the stable α phase already occurs between 160°C and 240°C, whereas the transition of sputtered β tantalum to the body-centred cubic phase occurs at about 800°C.[9]

The deposition of the tantalum at substrate temperatures above 160°C results in single-phase α tantalum films with a resistivity of 35 $\mu\Omega$ cm to 40 $\mu\Omega$ cm, which is somewhat higher than that of films crystallized from the amorphous phase. Their TCR ranges between 2500 ppm/K and 2800 ppm/K. The coarse-grained character of the originally amorphous films is, however, no longer attained. The grain diameter of the films is now 1 μm to 10 μm.

TABLE I
Dependence of structure and electrical properties of tantalum films on condensation temperature and subsequent heat treatment

substrate temperature during deposition (°C)	structure after deposition	structure after annealing	
		20°C, 2h	300°C, 2h
-160<T<-90	amorphous α=-60ppm/K ρ=230 μΩcm	α-Ta ρ=31 μΩcm α=3000ppm/K	α-Ta ρ=31 μΩcm α=3000ppm/K
-80 < T< 150	β-Ta ρ=240 μΩcm α=-200ppm/K	β-Ta ρ=240 μΩcm α=-200ppm/K	α-Ta ρ=35-45 μΩcm α=2600-2800 ppm/K
160<T<350	α-Ta ρ=35-40 μΩcm α=2500-2800ppm/K	—	α-Ta ρ=35-45 μΩcm α=2800-2800 ppm/K

temperature range for TCR: -160°C to 20°C
pressure during deposition and annealing: $<8\cdot10^{-7}$ N/m^2

In contrast to these results, high-vacuum deposition (10^{-3} N/m^2, substrate temperature 300°C) yielded fine-crystalline tantalum films with a resistivity of ρ_{20} = 60 $\mu\Omega$ cm and a temperature coefficient of α = 600 ppm/K.

Table I shows the dependence of the structure and the electrical properties of tantalum thin films on the deposition temperature and subsequent heat treatment in UHV.

3.2. *Tantalum-Nickel*

In order to stabilize the amorphous tantalum films, the attempt was undertaken to reduce the interaction between the tantalum atoms by alloying the tantalum with a second element. Nickel appeared suitable because at low temperatures, only a very small amount of nickel is dissolved in bulk tantalum (Figure 6).[10]

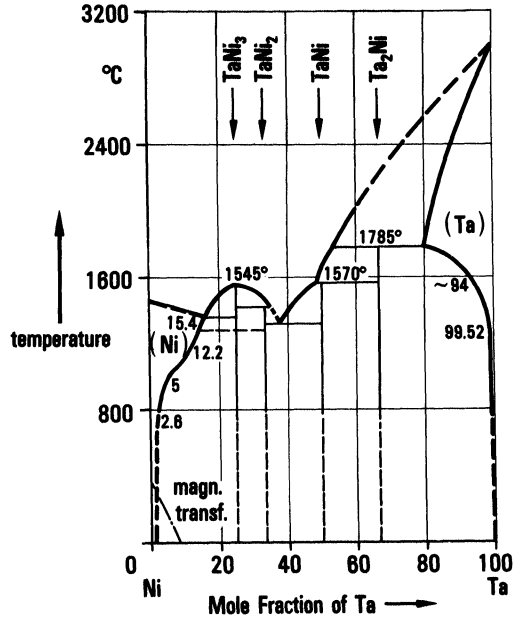

FIGURE 6 Phase diagram of tantalum-nickel 10.

In contrast to the tantalum films a pure nickel film deposited at −160°C exhibits no abrupt drop in resistivity when heated to room temperature. It may therefore be inferred that the nickel was already in its crystalline form when deposited. At room temperature the nickel film exhibits a fine-crystalline microstructure (Figure 7a). After heat treatment at 375°C for one hour the grain diameter expands to about 300 nm (Figure 7b). The film now has a

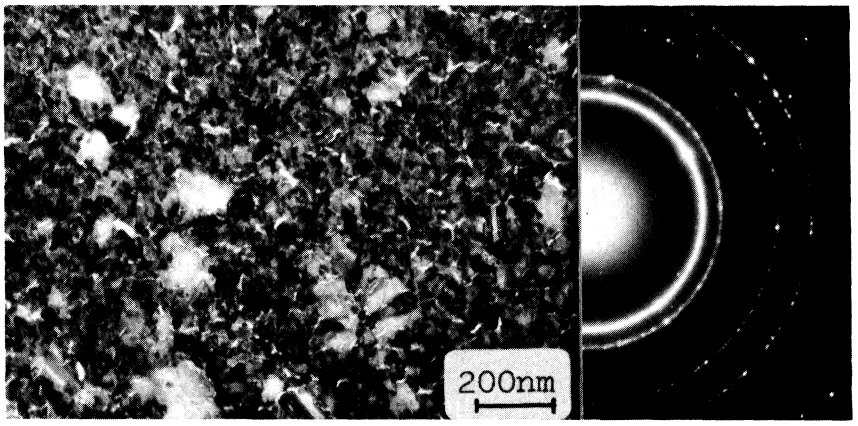

a)

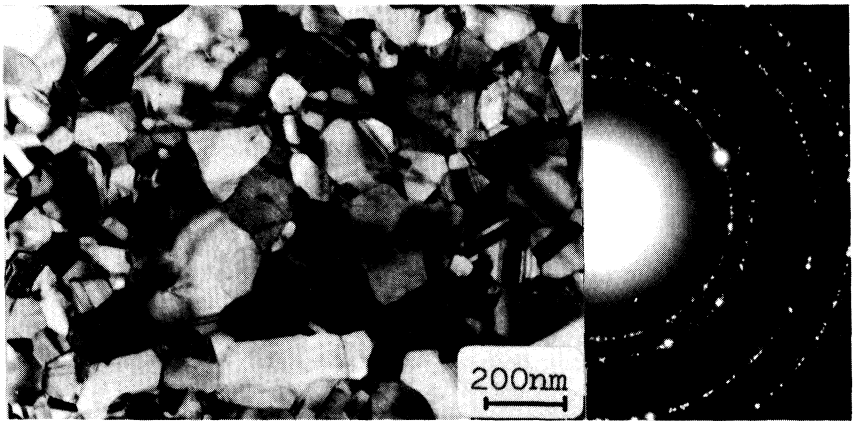

b)

FIGURE 7 Transmission electron micrographs and diffraction patterns of a nickel film (condensation temperature −160°C, film thickness d = 70 nm).

a) Film heated to room temperature.

b) Film annealed at 375°C in UHV for one hour.

reversible resistivity characteristic with a TCR of 3500 ppm/K, the resistivity being $\rho_{20} = 12.0\ \mu\Omega$ cm.

The addition of nickel during the deposition of the tantalum films (substrate temperature −160°C) brings about a radical change in their structure and electrical behaviour. The structure of tantalum-nickel films can be divided into different regions according to the added concentration of nickel (Figure 8).

In contrast to bulk tantalum (Figure 6) [10] up to a mole fraction of 8% nickel is dissolved in tantalum thin films.

Owing to the resistivity characteristic of these films in contrast to that of pure tantalum films, crystallization already begins at −150°C and continues for eight hours after room temperature is reached. Figure 9 shows the microstructure of an oriented grown film.

Although X-ray microstructure analyses indicate the presence of α tantalum, the lattice constant of $a_0 = 0{,}33058$ nm[11] is found to have dropped to 0,32873 nm, so indicating the incorporation of nickel atoms at lattice sites of the tantalum.

When the sample is heated to 400°C its resistivity of $\rho_{20} = 42\ \mu\Omega$cm is, as was to be expected, higher than that of pure α tantalum and its TCR is correspondingly lower at $\alpha = 1700$ ppm/K.

In the case of films with a concentration of a mole fraction of 8% to 20% nickel a mixture of α tantalum

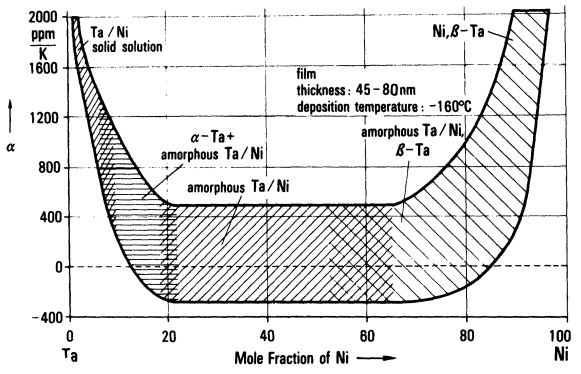

FIGURE 8 Temperature coefficient of resistivity of tantalum-nickel films as a function of the concentration of nickel.

and amorphous tantalum-nickel exists. The TCR ranges between +1200 ppm/K and −300 ppm/K depending on the phase distribution (Figure 8).

Tantalum-nickel films containing a mole fraction of 20% to 55% nickel (Figure 10a) do not display the interference lines of a crystalline substance in response to either electron diffraction (Figure 10b) or X-ray diffraction. The material has an amorphous structure. The TCR of the amorphous films varies between +500 ppm/K and −300 ppm/K (Figure 8), while their resistivity ranges between 130 $\mu\Omega$cm and 320 $\mu\Omega$cm.

Mole fractions of nickel exceeding 55% result in a mixture of amorphous tantalum-nickel and β tantalum. The amorphous phase vanishes as the nickel concentration is increased and β tantalum and nickel appear together. No formation of intermetallic phases between tantalum and nickel were observed even at temperatures up to 400°C.

4. DISCUSSION

The low stability of the UHV-deposited β tantalum films as compared to sputtered β tantalum[9] demonstrates the purity of the material. SIMS analyses show the thin films to contain no more impurities than the UHV-degassed starting materials (Marz grad tantalum and nickel). By taking account of the time needed to cover the substrate with a monolayer of absorbed gases (about 30 min at 10^{-7} N/m^2), and assuming a deposition rate of 0.2 nm/s, it is possible to estimate the incorporation of up to 10 ppm impurity atoms from the residual gas atmosphere.

Although the amorphous tantalum phase could not be detected electron-optically on account of its low crystallization temperature, its existence is indicated by various phenomena.

The crystallization of the tantalum films deposited at −160°C takes place within a narrow temperature range (Figure 2) and is accompanied by a drastic irreversible drop in resistivity. The drop in resistivity must be attributed to a phase transition, which does not exist for bulk tantalum.

As a phase transition, only the transition from an amorphous structure to crystalline α tantalum is possible, because the temperature range of existence for β tantalum could be determined very exactly (Figure 5, Table I).

In contrast to the bulk material nickel dissolves easily in UHV tantalum films deposited at −160°C (Figure 8 and Figure 9). This effect can only be explained by weak binding forces between the tantalum atoms, which could favour the existence of an amorphous state.

The experimental results further indicate that the

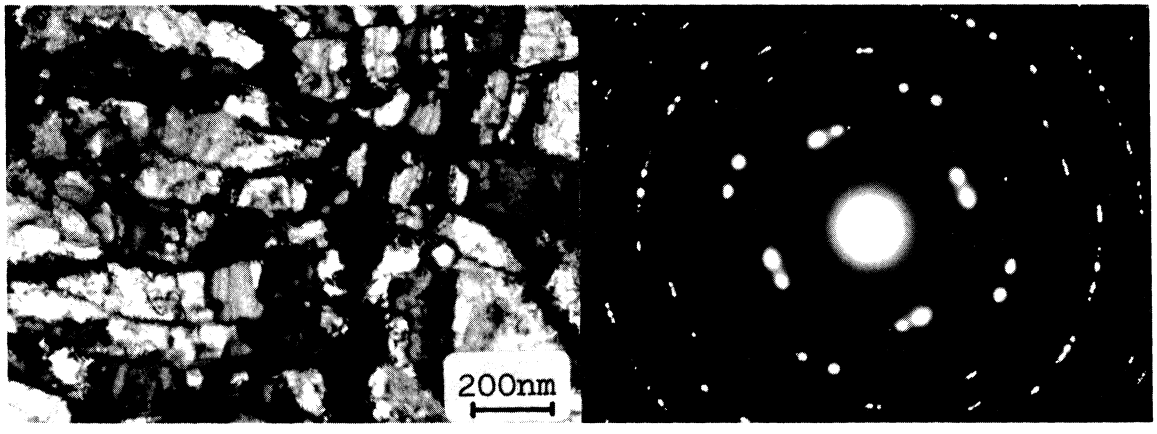

FIGURE 9 Transmission electron micrograph and diffraction pattern of a tantalum-nickel film (mole fraction of 2,4% nickel, condensation temperature −160°C, heated to room temperature).

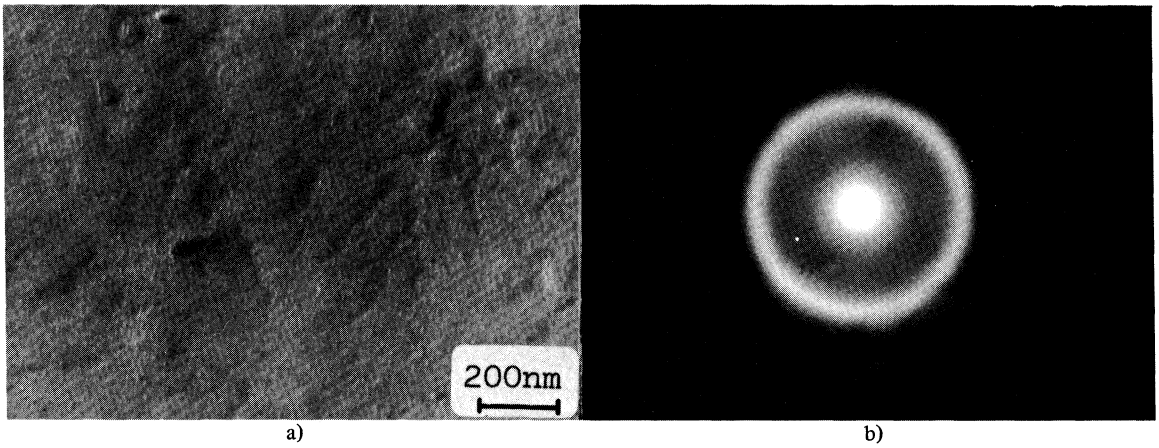

a) b)

FIGURE 10 Transmission electron micrograph and diffraction pattern of a tantalum-nickel film (mole fraction of 27% nickel, condensation temperature −160°C, heated to room temperature).
a) Transmission electron micrograph
b) Electron diffraction pattern

amorphous tantalum phase cannot be stabilized by adding less than a mole fraction of 8% nickel. The crystallization process, which already sets in at −150°C is greatly dependent on time and different from the abrupt transition of the amorphous tantalum phase to α tantalum (Figure 2).

Only by adding more than a mole fraction of 20% nickel amorphous tantalum-nickel films will be obtained. Such films exhibit the typical characteristics of amorphous metals, such as high resistivity (130 μΩcm to 320 μΩcm), diffuse electron diffraction patterns and contrastless electron microscopic transmission micrographs (Figure 10).

Since any influence of impurities can be excluded, the negative TCR of the amorphous tantalum films might be explained by an extrinsic conduction mechanism. The appearance of positive and negative TCRs in tantalum-nickel films (Figure 8) further indicates that different conduction mechanisms may also be present in the amorphous state. Whether this is due to different types of mechanism of short–range order needs to be clarified in further experiments.

REFERENCES

1. H. Jones, "Splat cooling and metastable phases," *Reports on Progress in Physics,* **36**, 1073 (1973), IV.
2. T. Ichikawa, "Electron diffraction study of the local atomic arrangement in amorphous Iron and Nickel films," *Phys. Stat. Sol. (a)*, **19**, 707 (1973).
3. H. A. Davies and J. B. Hull, "An amorphous phase in splat-quenched Al-17, 3 at% Cu alloy," *Script. Metallurgica,* **6**, 241 (1972).
4. U. Köster, P. Weiss, "Crystallization and decomposition of amorphous Silicon-Aluminium films," *J. of Non-Crystalline Solids,* **17**, 359 (1975).
5. S. Mader and A. S. Nowick, "Metastable Co–Au alloys: Example of an amorphous ferromagnet," *Appl. Phys. Letters*, 7, 3, 57 (1965).
6. P. Duwez, *"Phase stability in Metals and Alloys,"* McGraw-Hill Book Company, 1967.
7. V. J. Johnson, *"Properties of materials at low temperatures (Phase 1),"* Pergamon Press, p. 4, 151 (1961).
8. P. N. Baker, "Preparation and properties of Tantalum thin films," *Thin Solid Films,* **14**, 3 (1972).
9. N. Schwartz, W. A. Reed, P. Pollack and M. H. Read, "Temperature coefficient of resistance of Beta–Tantalum films and mixtures with B.C.C.–Tantalum," *Thin Solid Films,* **14**, 333 (1972).
10. F. A. Shunk, *"Constitution of Binary Alloys,"* McGraw-Hill Book Company, 1969.
11. Powder Diffraction File of the JCPDS. Card number 4-0788.